Stem Cell Research 16 (2016) 460–468

Contents lists available at ScienceDirect

Stem Cell Research

journal homepage: www.elsevier.com/locate/scr

Induced neural stem cells from distinct genetic backgrounds exhibit different reprogramming status

Sung Min Kim [a,b,1], Kyung Tae Lim [a,1], Tae Hwan Kwak [a,1], Seung Chan Lee [a], Jung Hyun Im [a], Sai Hali [a], Seon In Hwang [a], Dajeong Kim [c], Jeongho Hwang [b], Kee-Pyo Kim [d], Hak-Jae Chung [f], Jeong Beom Kim [g], Kinarm Ko [a,h], Hyung-Min Chung [a,h], Hoon Taek Lee [b], Hans R. Schöler [d,e], Dong Wook Han [a,h,*]

[a] Department of Stem Cell Biology, School of Medicine, Konkuk University, 1 Hwayang-dong, Gwangjin-gu, Seoul 143-701, Republic of Korea
[b] Department of Animal Biotechnology, Konkuk University, 1 Hwayang-dong, Gwangjin-gu, Seoul 143-701, Republic of Korea
[c] Dong-A Socio Holdings Research Center, 21, Geumhwa-ro 105 beon-gil, Giheung-gu, Yongin-si, Republic of Korea
[d] Department of Cell and Developmental Biology, Max Planck Institute for Molecular Biomedicine, Röntgenstraße 20, 48149 Münster, Germany
[e] University of Münster, Medical Faculty, Domagkstraße 3, 48149 Münster, Germany
[f] Animal Biotechnology Division, National Institute of Animal Science, RDA, Suwon 441-706, Republic of Korea
[g] School of Life Sciences, Ulsan National Institute of Science and Technology (UNIST), Ulsan, Republic of Korea
[h] KU Open-Innovation Center, Institute of Biomedical Science & Technology, Konkuk University, 1 Hwayang-dong, Gwangjin-gu, Seoul 143-701, Republic of Korea

ARTICLE INFO

Article history:
Received 30 September 2015
Received in revised form 18 January 2016
Accepted 8 February 2016
Available online 10 February 2016

Keywords:
Genetic backgrounds
Direct conversion
Direct reprogramming
Cell fate transition
iNSCs

ABSTRACT

Somatic cells could be directly converted into induced neural stem cells (iNSCs) by ectopic expression of defined transcription factors. However, the underlying mechanism of direct lineage transition into iNSCs is largely unknown. In this study, we examined the effect of genetic background on the direct conversion process into an iNSC state. The iNSCs from two different mouse strains exhibited the distinct efficiency of lineage conversion as well as clonal expansion. Furthermore, the expression levels of endogenous NSC markers, silencing of transgenes, and *in vitro* differentiation potential were also different between iNSC lines from different strains. Therefore, our data suggest that the genetic background of starting cells influences the conversion efficiency as well as reprogramming status of directly converted iNSCs.

1. Introduction

Recent studies in the stem cell field have demonstrated that cell fate transition could be achieved by introducing lineage-specific transcription factors with appropriate extrinsic signals. The ectopic expression of *Oct4*, *Sox2*, *Klf4*, and *c-Myc* with distinct culture conditions could induce either an embryonic stem cell- (Takahashi and Yamanaka, 2006) or epiblast stem cell-like state (Han et al., 2011) on somatic cells. Moreover, the different combinations of cell type specific transcription factors could directly convert the somatic cells not only into distinct somatic cell types such as dopaminergic neurons, endothelial cells, cardiomyocytes, embryonic sertoli-like cells, motor neurons, and hepatocytes (Buganim et al., 2012; Caiazzo et al., 2011; Huang et al., 2011; Ieda et al., 2010; Margariti et al., 2012; Sekiya and Suzuki, 2011; Son et al., 2011) but also the self-renewing somatic stem cells or progenitor cells including definitive endoderm-like cells, neural crest cells, neuroepithelial progenitors, cardiac progenitors, and hepatic stem cells (Li et al., 2014; Kim et al., 2014a; Lu et al., 2013; Efe et al., 2011; Yu et al., 2013).

Although previous studies have developed a variety of technologies to directly convert somatic cells into distinct cell types, the conversion efficiency into the target cell types is very low. Therefore, to facilitate the cell fate transition into distinct cellular identities and also to understand the underlying mechanisms of lineage transition, many previous studies screened factors boosting or inhibiting cell fate transition, such as epigenetic modifiers, chromatic remodeling complexes, microenvironments, additional transcription factors, non-transcription factors, and genetic backgrounds. First, the early chemical screening studies revealed the inhibitory factors including histone methyltransferases, DNA methyltransferases, and histone deacetylases whose inhibition by small molecules could improve the reprogramming efficiency into iPSCs (Shi et al., 2008; Mikkelsen et al., 2008; Huangfu et al., 2008). Second, the boosting effects of chromatin remodeling complexes, DNA hydroxylase and its associated factor, and even basic transcription machinery have been also well documented throughout previous

Abbreviations: iNSCs, induced neural stem cells; iPSCs, induced pluripotent stem cells; iEpiSCs, induced epiblast stem cells; MEFs, mouse embryonic fibroblasts; qPCR, quantitative polymerase chain reaction; cNSCs, control neural stem cells.

* Corresponding author at: Department of Stem Cell Biology, School of Medicine, Konkuk University, 1 Hwayang-dong, Gwangjin-gu, Seoul 143-701, Republic of Korea.
E-mail address: dwhan@konkuk.ac.kr (D.W. Han).

[1] These authors contributed equally to this work.

http://dx.doi.org/10.1016/j.scr.2016.02.025

reprogramming studies (dos Santos et al., 2014; Singhal et al., 2010; Gao et al., 2013; Doege et al., 2012; Pijnappel et al., 2013). Third, the effects of microenvironment such as hypoxia condition, soluble factors including Vitamin C, and the metabolic switch from the somatic state into the pluripotent state were also carefully investigated during the iPSC generation (Yoshida et al., 2009; Esteban et al., 2010; Mathieu et al., 2014). Fourth, the additional transcription factors and also non-transcription factors even including microRNAs in combination with *Oct4*, *Sox2*, *Klf4*, and *c-Myc* also displayed a positive effect on the induction of pluripotency (Buganim et al., 2014; Han et al., 2010; Hanna et al., 2008; Maekawa et al., 2011; Redmer et al., 2011; Subramanyam et al., 2011). Finally, the genetic background could also influence the induction and maintenance of pluripotency (Schnabel et al., 2012; Hanna et al., 2009). However, the effects of the above-mentioned additional genetic and epigenetic factors on the direct conversion into distinct somatic cell fates are largely unknown.

We have previously shown that the ectopic expression of *Brn4*/*Pou3f4*, *Sox2*, *Klf4* and *c-Myc* (BSKM) could enable the direct conversion of mouse embryonic fibroblasts (MEFs) into a neural stem cell (NSC)-like state, namely induced NSCs (iNSCs) (Han et al., 2012; Kim et al., 2014b). The directly converted iNSCs closely resemble control NSCs from brain-tissue in terms of the gene expression pattern, epigenetic status, self-renewal capacity and their *in vitro* and *in vivo* differentiation potential (Han et al., 2012; Kim et al., 2014b). Furthermore, iNSCs exhibited the therapeutic potential after transplantation into disease model without forming tumor up to 6 months (Hong et al., 2014; Hemmer et al., 2014), suggesting the potential clinical application of iNSCs in neuronal diseases. However, our previous studies demonstrated the iNSC generation only using MEFs from the C3H mouse strain background (Han et al., 2012; Kim et al., 2014b).

In the current study, we compared two different genetic backgrounds on the induction and maintenance of multipotency by generating clonal iNSC lines from two distinct mouse strains (C57BL/6 *vs.* C3H). Clonal iNSC lines from distinct genetic backgrounds exhibited the distinct levels of conversion efficiency, endogenous NSC markers, transgene expression, and *in vitro* differentiation although iNSC lines from both strains shared typical features of NSCs such as morphology, gene expression pattern, and epigenetic status, indicating that the genetic backgrounds influence the cell fate transition into an iNSC state. In addition, the comparative analysis of clonal iNSC lines could serve as a platform for screening the most suitable and functional iNSC line for clinical translation of direct conversion technology.

2. Materials and methods

2.1. Cell culture

Mouse embryonic fibroblasts (MEFs) were isolated from C57BL/6 and C3H mouse strains on E13.5 after carefully removing the head, spinal cord, and all the internal organs. MEFs were maintained in DMEM (Biowest) containing 10% fetal bovine serum (FBS) (Biowest), 1× MEM/NEAA (Gibco), and 1× penicillin/streptomycin/glutamine (Invitrogen). Both NSCs and iNSCs were maintained in neural stem cell medium (NSM): DMEM/F-12 (Gibco) containing, 1× B27 supplements (Gibco), 1× penicillin/streptomycin/glutamine (Invitrogen), 0.05% BSA fraction V (Invitrogen), 10 ng/ml of basic fibroblast growth factor (bFGF) (Peprotech), and 10 ng/ml of epidermal growth factor (EGF) (Peprotech).

2.2. Retrovirus production

The retroviral particles were produced by transfection of pMXs vectors into Platinum E cells (Plat-E cells, Cell Biolabs). Briefly, 9 μg of pMXs vectors was transfected into the Plat-E cells using 27 μl of FuGENE 6 transfection reagent (Promega). After 48 h, the supernatants containing viral particles were carefully collected and filtered through a 0.22-μm syringe filter (Minisart).

2.3. Generation of iNSCs

For generating iNSCs, 5×10^4 MEFs were plated onto gelatin-coated 35 mm cell culture dish. Next day, MEFs were transduced with retroviral particles encoding BSKM and cultured as previously described (Han et al., 2012; Kim et al., 2014b). Briefly, the transduced MEFs were maintained in NSM, which was replaced with fresh medium every other day until the initial clusters were observed. Once the initial clusters become mature, whole cells were split in a 1:1 ratio for the iNSC expansion.

2.4. Establishment of clonal iNSC lines

For establishment of clonal iNSC lines, FACS-mediated single cell sorting was performed at 6 weeks after viral transduction. The iNSCs were carefully dissociated with Trypsin/EDTA (Gibco), and collected with DMEM (Biowest) containing 10% FBS, and then washed with PBS (Biowest). The cells were incubated with FITC-conjugated SSEA1 antibody (Santa Cruz Biotechnology, 1:10) for 15 min at room temperature. The SSEA1-positive single cells were sorted using BD FACSAria™ (BD Biosciences) and plated onto laminin/poly-D-lysine–coated 96-well plates. To measure the cell survival, the expanded colonies were counted 10 days after sorting. Three clonal iNSC lines from each strain were expanded and maintained for comparative analysis.

2.5. RT-PCR and qPCR

Total RNA was isolated from samples by using the Hybrid-R™ RNA isolation kit (GeneAll) according to the manufacturer's protocol. 1 μg of isolated RNA was converted to complementary DNA (cDNA) using the High Capacity cDNA Reverse Transcription Kit (Applied Biosystems). RT-PCR was performed using the GoTag green master mix (Promega). qPCR was performed using SYBR green PCR Master Mix (Applied Biosystems) on the ABI 7500 real-time PCR system (Applied Biosystems). ΔCt values were calculated by subtracting *Gapdh* Ct value from that of each target genes. Relative expression levels were calculated by using $2^{-\Delta\Delta Ct}$ methods. The primer sets used are listed in Supplementary Table S1.

2.6. Bisulfite sequencing

To investigate the DNA methylation status in clonal iNSC lines, bisulfite sequencing was performed using EpiTect Bisulfite Kit (QIAGEN). All unmethylated cytosine residues in genomic DNA were converted into uracil residues upon sodium bisulfite treatment. SuperTaq polymerase (Ambion) was used for PCR amplifications. For nested PCR, 3 μl of the product from the first round of PCR was used as a template for second round PCR. The amplified products were extracted after electrophoresis on 1% agarose gels and subcloned into the pCR2.1®-TOPO® TA vector (Invitrogen) according to the manufacturer's protocol. The QIAprep Spin Miniprep Kit (QIAGEN) was used to purify the subcloned plasmids. Individual clones were sequenced (Macrogen, Korea) and analyzed using QUMA software (http://quma.cdb.riken.jp). The primer sets used are listed in Supplementary Table S2.

2.7. Immunocytochemistry

The cells were fixed with 4% paraformaldehyde (Chemcruz) for 30 min at room temperature, and then washed 3 times with PBS (Biowest). After washing, the fixed cells were then permeabilized and blocked with PBS containing 0.03% Triton X-100 (Sigma Aldrich) and 5% FBS (Biowest) for 1 h at room temperature. The following primary antibodies were used: mouse anti-NESTIN (Millipore, 1:200), goat

anti-SOX2 (Santa Cruz Biotechnology, 1:200), rabbit anti-OLIG2 (Millipore, 1:200), mouse anti-SSEA1 (Santa Cruz Biotechnology, 1:100), mouse anti-TUJ1 (Covance, 1:500), rabbit anti-GFAP (Dako, 1:500), and rat anti-MBP (Abcam, 1:100). Cells were incubated with primary antibodies for 16 h at 4 °C, washed three times with PBS, and incubated with secondary antibodies for 2 h at room temperature. The following secondary antibodies were used: Alexa Fluor 488 rabbit anti-goat IgG (Invitrogen, 1:1000), Alexa Fluor 568 rabbit anti-mouse IgG (Invitrogen, 1:1000), Alexa Fluor 568 goat anti-rabbit IgG (Invitrogen, 1:1000), Alexa Fluor 488 donkey anti-rabbit IgG (Invitrogen, 1:1000), and Alexa Fluor 568 goat anti-rat IgG (Invitrogen, 1:1000). Nuclei were counter-stained with Hoechst 33342 (Invitrogen).

2.8. In vitro differentiation of iNSCs

For neuron differentiation, iNSCs were dissociated into single cells and 5×10^4 cells were plated onto laminin/poly-D-lysine–coated 4-well plates. After 24 h, the medium was replaced with neural differentiation medium: DMEM/F-12 (Gibco) containing 1× B27 supplements (Gibco), 1× penicillin/streptomycin/glutamine (Invitrogen), and 10 ng/ml bFGF. 4 days after differentiation, the neural maturation medium containing 200 mM ascorbic acid (Sigma) without growth factors was supplied for 8–10 more days. For astrocyte differentiation, iNSCs were cultured in DMEM/F-12 (Gibco) supplemented with 10% FBS and 1× penicillin/streptomycin/glutamine on gelatin-coated dishes for 5 days. For oligodendrocyte differentiation, 5×10^4 cells of iNSCs were plated onto laminin/poly-D-lysine-coated 4-well plates. After 24 h, the medium was replaced with oligodendrocyte differentiation medium: DMEM/F-12 (Gibco) containing 1× B27 supplements, 1× penicillin/streptomycin/glutamine, 10 ng/ml bFGF, and 10 ng/ml PDGF (Sigma). 4 days after differentiation, the oligodendrocyte maturation medium containing 30 ng/ml T3 (Sigma) and 200 mM ascorbic acid without growth factors was supplied for another 4 days. The medium was replaced with fresh medium daily.

3. Results

3.1. Genetic background influences iNSC generation

In order to examine the effect of genetic background on iNSC generation, we derived mouse embryonic fibroblasts (MEFs) from C3H and C57BL/6 mouse strains (see Fig. 1A). Both MEFs displayed typical fibroblast morphology with similar gene expression patterns and proliferation rates (Fig. 1B, C). We next transduced retroviruses encoding *Brn4*, *Sox2*, *Klf4*, and *c-Myc* (BSKM) into these MEFs. The quantitative polymerase chain reaction (qPCR) analysis indicated that the expression levels of all transgenes were similar between MEFs derived from the two strains (Fig. 1D). We then cultured the transduced MEFs under NSC-promoting conditions. As the initial iNSCs can be defined by SSEA1 expression (Kim et al., 2014b), we compared the conversion efficiency into an iNSC state by estimating the proportion of SSEA1-positive cells from the entire transduced MEFs at 6 weeks post-infection. Compared to C57BL/6 MEFs that showed less than 3% of SSEA1-positive cells, more than 8% of SSEA1-positive cells were observed on the C3H MEFs. These data indicate that the genetic background influences the conversion efficiency into an iNSC state (Fig. 1E).

3.2. Genetic background influences the survival rate of clonal iNSCs

We previously described that bulk culture of early-passage iNSCs is a heterogeneous population comprised of non-reprogrammed somatic cells, partially reprogrammed cells, and fully reprogrammed iNSCs (Kim et al., 2014b). Thus, to evaluate and compare the reprogramming status of iNSCs derived from two distinct mouse strains, we next generated clonal iNSC lines from both strains by sorting SSEA1-positive single cells into 96-well plates. For the fair comparison, we sorted SSEA1-positive cells from two independently transduced MEFs per each strain and established three clonal iNSC lines from each strain. They all exhibited morphology similar to that of control NSCs (cNSCs) derived from brain-tissues (Fig. 1G). Notably, the survival rate of SSEA1-positive single cells was significantly different between the two strains (C57BL/6: 6.9% ± 1.6% *vs.* C3H: 12.2% ± 2.2%) (Fig. 1F). Thus, these data suggest that the genetic background also influences the survival rate of single cell-sorted early stage iNSCs.

3.3. iNSCs from distinct genetic backgrounds exhibit different reprogramming status.

All the clonal iNSC lines from both strains expressed typical NSC markers such as SOX2, NESTIN, OLIG2, and SSEA1 as evidenced by immunostaining (Fig. 2A and Fig. S1). Furthermore, bisulfite sequencing analysis revealed that all the clonal iNSC lines showed the promoter DNA methylation patterns similar to those of cNSCs, but clearly distinct from those of starting MEFs. Specifically, the regulatory region of *Nestin* became demethylated in the iNSC lines, and its methylation levels were similar in iNSCs and cNSCs (Fig. 2B, C and Fig. S2). The promoter of *Col1a1*, a fibroblast marker, was dramatically *de novo* methylated in the iNSC lines to a level similar to that of cNSCs. DNA methylation patterns at these two loci were correlated with their gene expression status (Fig. 3A). These data suggest that all the iNSC clones generated from both mouse stains were reprogrammed into a NSC-like state at both the transcriptional and epigenetic levels.

To further characterize the iNSC clones, we next investigated the expression levels of NSC and fibroblast markers using qPCR analysis (Fig. 3A). All clones generated from both strains exhibited activation of the endogenous NSC markers such as *Pax6*, *Nestin*, *Olig2*, *Mash1*, *Blbp*, *Brn2*, *Sox3* and *Msi1* with complete inactivation of the fibroblast markers, *Thy1*, *Col1a1*, *and Pdgfrb*. Interestingly, *Sox2*, a representative NSC marker, was highly activated in all C3H iNSC clones, whereas it was barely detectable in all C57BL/6 iNSC clones despite of the strong expression of Sox2 at a protein level (Fig. 2A and Fig. S3). To understand this discrepancy, we investigated the integration of all transgenes and their expression patterns in all clones. Genomic PCR analysis indicated that all transgenes were integrated into the genome of all clones (Fig. 3B). qPCR analysis showed a complete silencing of BSKM in the C3H iNSC clones. However, transgenic *Sox2* but not the other transgenes was still highly expressed in all C57BL/6 iNSC clones (Fig. 3C). The residual expression of exogenous *Sox2* may explain the discrepancy between the levels of Sox2 transcript and protein. Thus, iNSC clones derived from C57BL/6 MEFs were partially transgene-dependent. Taken together, our data show that C57BL/6 MEFs are less susceptible to the conversion process toward an iNSC state and also that the endogenous NSC transcriptional program is less well established in the C57BL/6 iNSC clones than in C3H iNSC clones.

3.4. Distinct in vitro differentiation potential of iNSCs derived from two genetic backgrounds

As the reprogramming status of the iNSC clones derived from the two mouse strains differed in terms of their gene expression patterns of both endogenous and exogenous NSC markers, we next investigated if iNSCs from the two strains have distinct levels of their differentiation ability. To this end, we induced *in vitro* differentiation of all iNSC clones from both C57BL/6 and C3H strains into neurons, astrocytes, and oligodendrocytes. As in our previous studies, iNSC clones derived from C3H MEFs could differentiate into all three neuronal lineages including neurons, astrocyte, and oligodendrocytes, as evidenced by the immunostaining with antibodies against TUJ1, GFAP, and MBP, respectively (Fig. 4A, B, C). Notably, the differentiation potential of C3H iNSC clones into both neurons and astrocytes was nearly comparable to that of cNSCs, although they rarely differentiated into oligodendrocytes

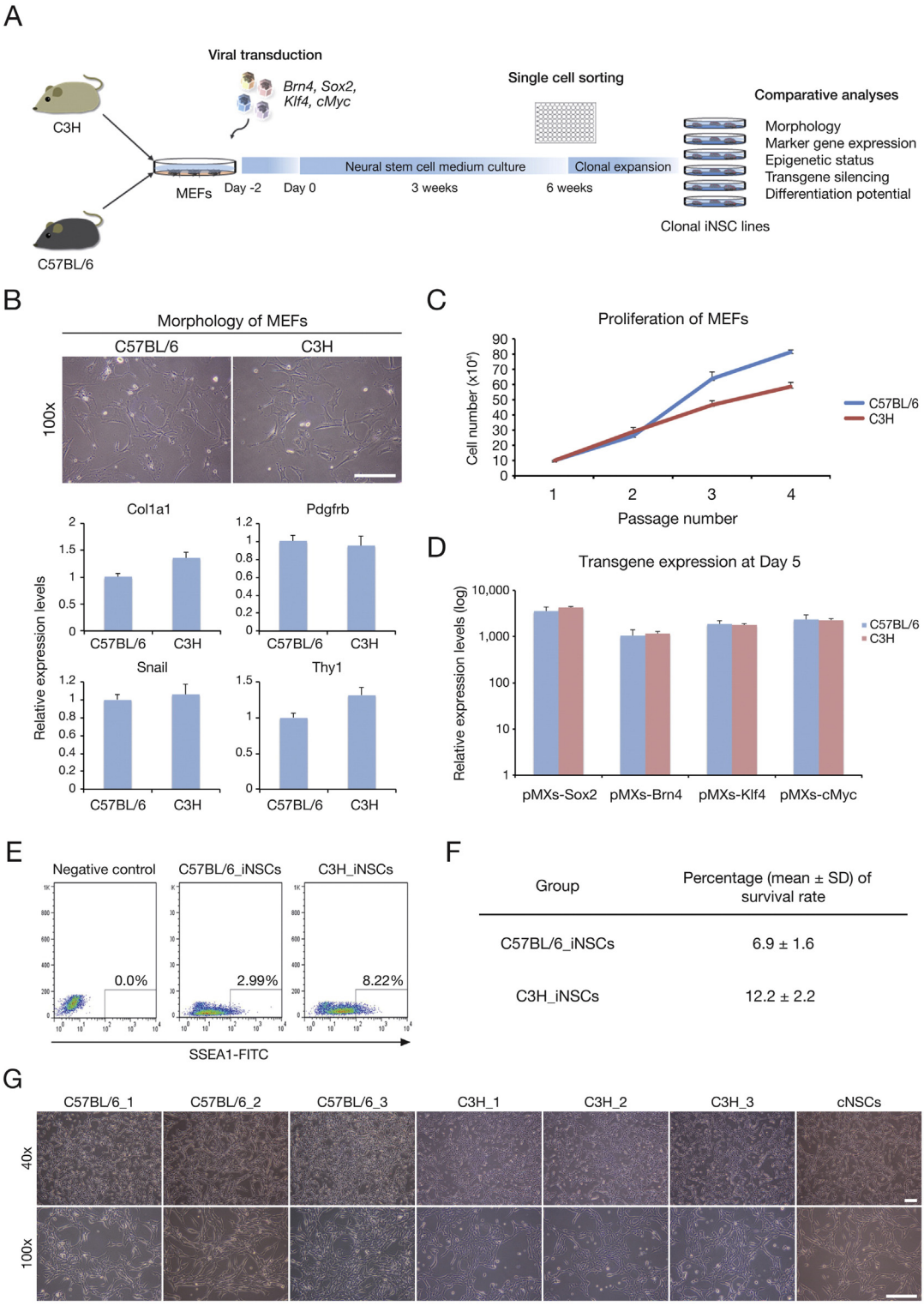

Fig. 1. Generation of iNSCs from different genetic backgrounds. (A) Schematic illustration showing the procedure for the direct conversion of C57BL/6 and C3H MEFs into iNSCs. (B) Morphology and marker expression of MEFs. Scale bar, 200 μm. Error bars indicate standard deviation ($n = 3$). (C) The proliferation of MEFs. MEFs were passaged every other day in 12-well plates (1×10^5 cells per well). (D) Expression levels of transgenes in MEFs were analyzed by qPCR on day 5 after infection. Expression levels are normalized to those of untransduced MEFs. Error bars indicate standard deviation ($n = 3$). (E) The efficiency of iNSC generation was determined by FACS analysis using antibody against SSEA1 at 6 weeks after viral transduction. MEFs were used as a negative control. (F) The survival rate of iNSCs derived from C57BL/6 and C3H strains after single cell sorting into poly-D-Lysine coated 96-well plates. Data are presented as mean ± standard deviation. (G) Morphology of the established clonal iNSC lines derived from C57BL/6 and C3H strains at passage 10. Scale bars, 200 μm.

compared to cNSCs (Fig. 4C), in agreement with our previous studies (Han et al., 2012; Kim et al., 2014b; Hong et al., 2014) where we also observed this biased differentiation pattern of C3H iNSCs. In contrast to C3H iNSCs, all iNSC clones derived from C57BL/6 MEFs exhibited a significantly impaired differentiation potential into both neurons and astrocytes (Fig. 4A, B). Furthermore, C57BL/6 iNSCs also showed limited differentiation into oligodendrocytes, similar to C3H iNSC clones (Fig. 4C). Although the oligodendrocytes from C3H iNSC clones

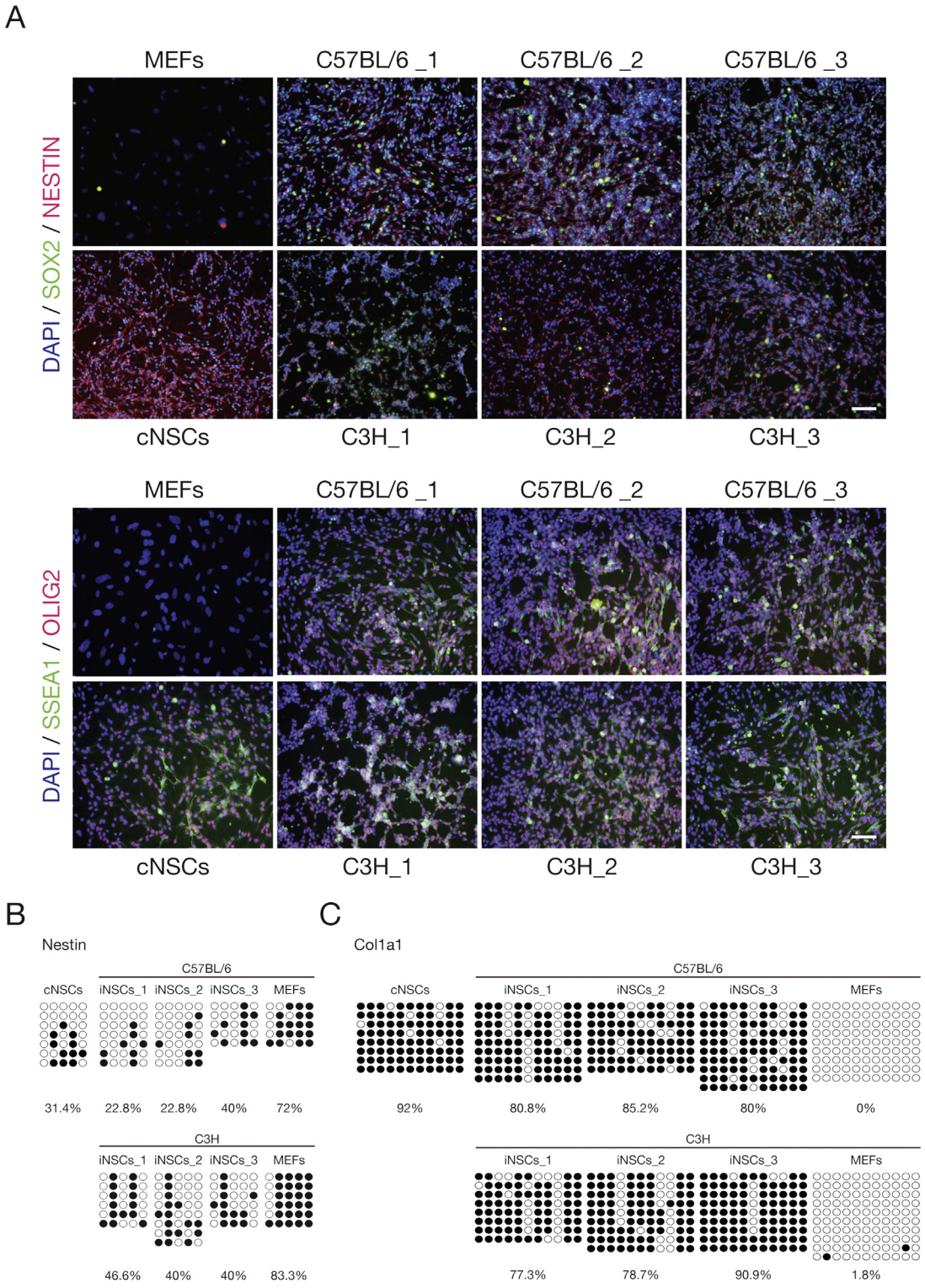

Fig. 2. Comparative analysis of clonal iNSC lines derived from the two mouse strains. (A) Immunofluorescence microscopy images of clonal iNSC lines using antibodies against SOX2, NESTIN, OLIG2, and SSEA1. MEFs and control NSCs were used as negative and positive control, respectively. Scale bars, 200 μm. (B, C) DNA methylation status of the second intron of *Nestin* and promoter region of *Col1a1* in clonal iNSC lines from C57BL/6 and C3H strains was assessed by bisulfite sequencing PCR. MEFs and control NSCs were served as negative and positive control, respectively. Open and filled circles represent unmethylated and methylated CpGs, respectively.

displayed the relatively mature and defined structures, we rarely detected the matured oligodendrocytes from C57BL/6 iNSCs under the identical differentiation condition. All together, our data indicate that the genetic background influences the functionality of directly converted iNSCs.

4. Discussion

To understand the mechanism underlying the induction of pluripotency, a number of inhibiting and boosting factors have been identified throughout screening multiple epigenetic and genetic factors

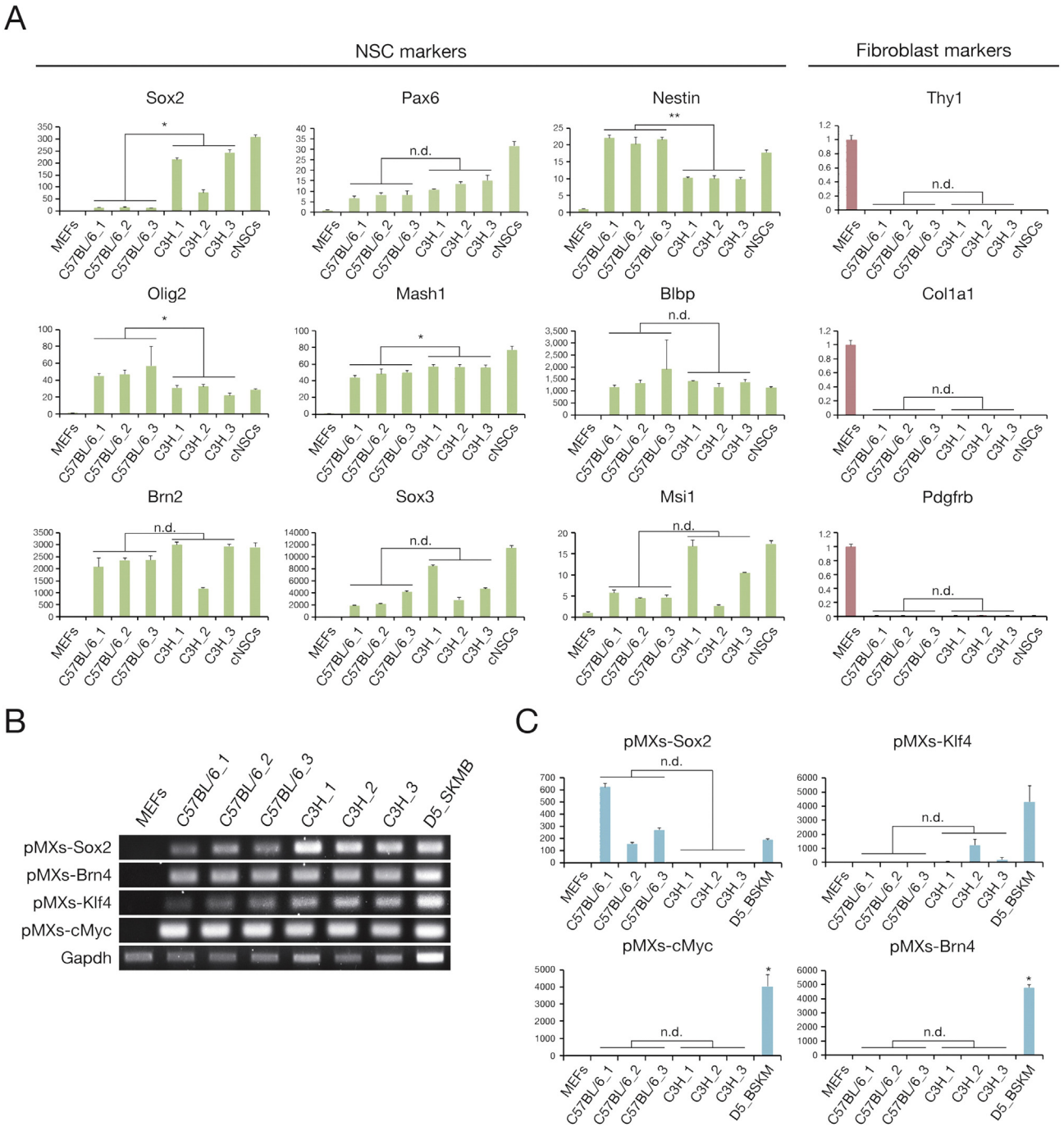

Fig. 3. Gene expression status of clonal iNSC lines derived from two mouse strains. (A) Expression of NSC and fibroblast markers in clonal iNSC lines analyzed by qPCR. The expression levels are normalized to those of MEFs. Error bars indicate the standard deviation ($n = 3$). (B) Genomic integration of transduced reprogramming factors was examined by genomic PCR. (C) Expression levels of exogenous reprogramming factors in clonal iNSC lines at passage 20 were examined by qPCR. BSKM-transduced MEFs at day 5 post-infection were used as a positive control. Error bars indicate the standard deviation ($n = 3$).

potentially influencing iPSC generation. However, the factors that positively or negatively affect the induction of multipotency or unipotency *via* the direct conversion process, remain elusive. In this study, we tried to elucidate the effect of the genetic background on the induction and maintenance of iNSCs.

Although we were able to generate stably expandable iNSC lines from both mouse strains tested (C57BL/6 and C3H), these iNSC lines exhibited substantial differences in both the induction and maintenance phases of multipotency. First, the conversion efficiency as assessed by the number of SSEA1-positive population was significantly different between the two mouse strains. Furthermore, iNSCs from the C57BL/6 strain showed relatively poor induction of an iNSC state, as evidenced by impaired activation of endogenous *Sox2* and incomplete silencing of transgenic *Sox2*. Thus, these data suggest that the genetic background influences the induction of multipotency in a neuronal lineage. Second, the survival rates of sorted SSEA1-positive single cells was also significantly different between iNSC clones from the two strains, indicating that the maintenance of iNSC identity after successful conversion into the SSEA1-positive iNSC state is also influenced by the genetic backgrounds. Moreover, all clonal iNSC lines derived from C57BL/6 strain displayed the limited *in vitro* differentiation potential into neurons,

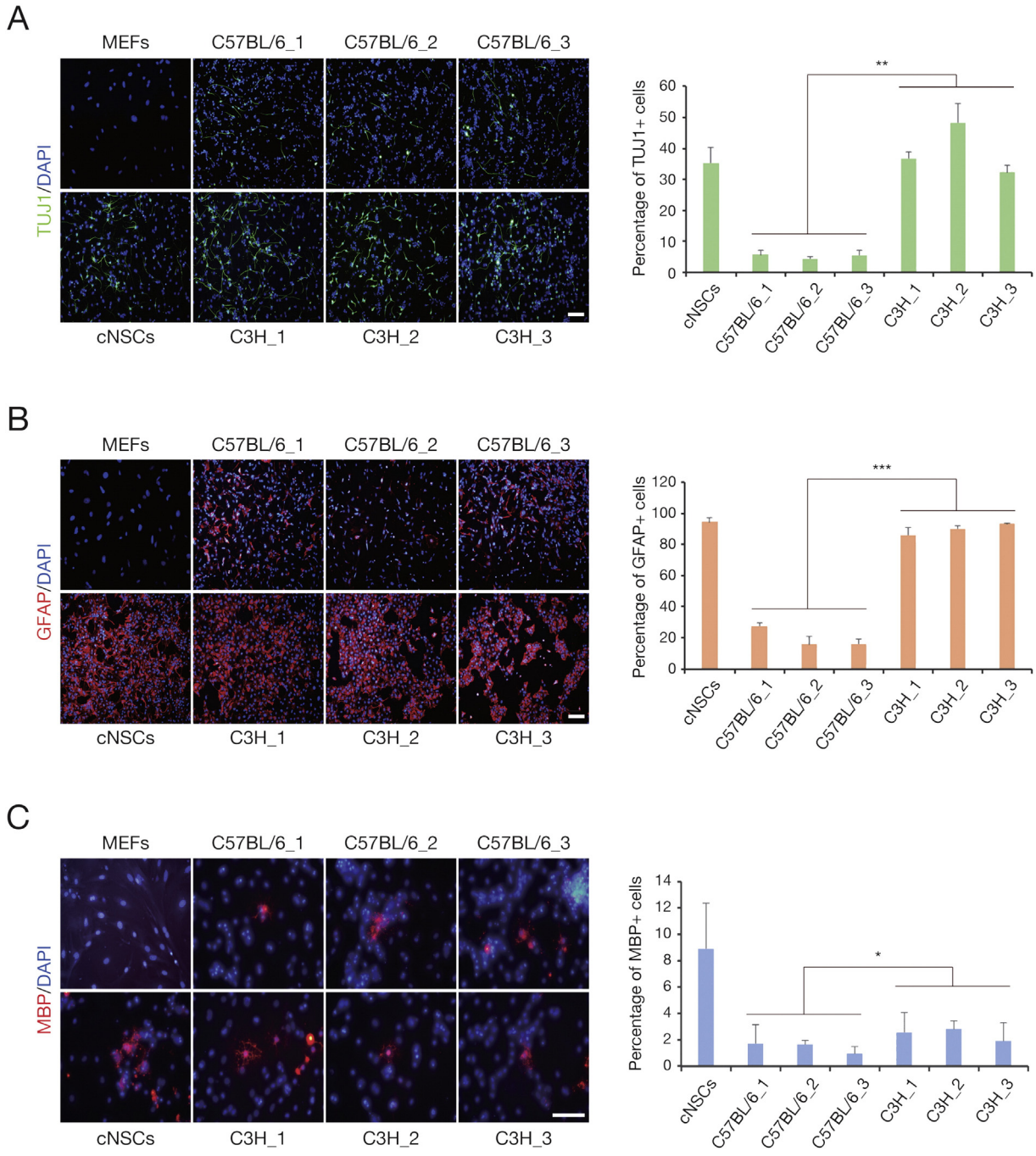

Fig. 4. *In vitro* differentiation potential of clonal iNSC lines derived from two mouse strains. (A–C) Differentiation potential of clonal iNSC lines into neurons (A) astrocytes (B) and oligodendrocytes (C) as shown by immunostaining with antibodies against TUJ1, GFAP, and MBP, respectively. The efficiency of differentiation was examined by quantifying the numbers of TUJ1-, GFAP-, and MBP-positive cells against nuclear staining. Control NSCs were used as a positive control for determining the differentiation efficiency. Scale bars, 100 μm.

astrocytes, and oligodendrocytes, indicating that the functionality of the iNSCs was also impaired in C57BL/6 iNSCs.

We observed the abnormally increased proliferation of C57BL/6 iNSC clones compared to C3H iNSCs and cNSCs (data not shown). In the previous study (Graham et al., 2003), it was demonstrated that the ectopic expression of *Sox2* could induce increased proliferation and also block the proper differentiation of NSCs into their daughter cell types. Thus, the increased proliferation rate and impaired differentiation ability of C57BL/6 iNSCs can be explained by the residual expression of exogenous *Sox2* in C57BL/6 iNSCs (Fig. 2A, Fig. 3C and Fig. S3). It would be interesting to further decipher the mechanism governing the strain-dependent regulation of both the endogenous NSC program and transgenes, which might be tightly linked to the functionality of iNSCs. Finally, it would be also interesting to examine whether the effect of the genetic background on the induction and maintenance of other cell types (*e.g.* induced hepatocytes and induced neurons) directly converted from somatic cells by defined transcription factors.

Recent studies have described that the distinct combinations of transcription factors can induce direct conversion of various human cells into an iNSC-like state (Lu et al., 2013; Ring et al., 2012; Wang et al., 2013; Yu et al., 2015; Zhu et al., 2014). Although the data provided in these studies support the cellular identity of human iNSCs, their molecular and functional features were not precisely characterized at the clonal level. Therefore, comparing the induction and maintenance of the NSC fate on human somatic cells at the clonal level might allow

us to elucidate the underlying mechanism of direct conversion into NSCs.

5. Conclusion

In this study, we established iNSCs from two different mouse strains (C3H and C57BL/6). These two iNSCs exhibited distinct reprogramming status in terms of NSC markers expression, silencing of transgenes, and *in vitro* differentiation potential. Our data suggest that the genetic backgrounds influence the induction and maintenance of directly converted iNSCs. This is the first report describing the effects of genetic backgrounds on the cell fate transition into an iNSC state.

Conflict of interest

The authors declare that they have no conflicts of interest with the contents of this article.

Author contributions

S.M.K., K.T.L., and T.H.K. performed most of the experiments. S.C.L., J.H.I., S.H. measured the expression level of SOX2 protein. J.H., S.I.H. performed the DNA methylation analysis and proliferation assay. H.C., D.K., H.T.L., and K.K. performed functional assay of iNSCs. K.K., H.C., and H.R.S. edited the manuscript. D.W.H. conceived the project and wrote the manuscript.

Acknowledgments

This research was supported by the Basic Science Research Program through the National Research Foundation of Korea (NRF), funded by the Ministry of Education, Science and Technology (2011-0013885) and also by Korea Health Technology R&D Project, Ministry of Health & Welfare Grant A120392.

Appendix A. Supplementary data

Supplementary data to this article can be found online at http://dx.doi.org/10.1016/j.scr.2016.02.025.

References

Buganim, Y., Itskovich, E., Hu, Y.C., Cheng, A.W., Ganz, K., Sarkar, S., Fu, D., Welstead, G.G., Page, D.C., Jaenisch, R., 2012. Direct reprogramming of fibroblasts into embryonic Sertoli-like cells by defined factors. Cell Stem Cell 11, 373–386.

Buganim, Y., Markoulaki, S., van Wietmarschen, N., Hoke, H., Wu, T., Ganz, K., Akhtar-Zaidi, B., He, Y., Abraham, B.J., Porubsky, D., Kulenkampff, E., Faddah, D.A., Shi, L., Gao, Q., Sarkar, S., Cohen, M., Goldmann, J., Nery, J.R., Schultz, M.D., Ecker, J.R., Xiao, A., Young, R.A., Lansdorp, P.M., Jaenisch, R., 2014. The developmental potential of iPSCs is greatly influenced by reprogramming factor selection. Cell Stem Cell 15, 295–309.

Caiazzo, M., Dell'Anno, M.T., Dvoretskova, E., Lazarevic, D., Taverna, S., Leo, D., Sotnikova, T.D., Menegon, A., Roncaglia, P., Colciago, G., Russo, G., Carninci, P., Pezzoli, G., Gainetdinov, R.R., Gustincich, S., Dityatev, A., Broccoli, V., 2011. Direct generation of functional dopaminergic neurons from mouse and human fibroblasts. Nature 476, 224–227.

Doege, C.A., Inoue, K., Yamashita, T., Rhee, D.B., Travis, S., Fujita, R., Guarnieri, P., Bhagat, G., Vanti, W.B., Shih, A., Levine, R.L., Nik, S., Chen, E.I., Abeliovich, A., 2012. Early-stage epigenetic modification during somatic cell reprogramming by Parp1 and Tet2. Nature 488, 652–655.

dos Santos, R.L., Tosti, L., Radzisheuskaya, A., Caballero, I.M., Kaji, K., Hendrich, B., Silva, J.C., 2014. MBD3/NuRD facilitates induction of pluripotency in a context-dependent manner. Cell Stem Cell 15, 102–110.

Efe, J.A., Hilcove, S., Kim, J., Zhou, H., Ouyang, K., Wang, G., Chen, J., Ding, S., 2011. Conversion of mouse fibroblasts into cardiomyocytes using a direct reprogramming strategy. Nat. Cell Biol. 13, 215–222.

Esteban, M.A., Wang, T., Qin, B., Yang, J., Qin, D., Cai, J., Li, W., Weng, Z., Chen, J., Ni, S., Chen, K., Li, Y., Liu, X., Xu, J., Zhang, S., Li, F., He, W., Labuda, K., Song, Y., Peterbauer, A., Wolbank, S., Redl, H., Zhong, M., Cai, D., Zeng, L., Pei, D., 2010. Vitamin C enhances the generation of mouse and human induced pluripotent stem cells. Cell Stem Cell 6, 71–79.

Gao, Y., Chen, J., Li, K., Wu, T., Huang, B., Liu, W., Kou, X., Zhang, Y., Huang, H., Jiang, Y., Yao, C., Liu, X., Lu, Z., Xu, Z., Kang, L., Chen, J., Wang, H., Cai, T., Gao, S., 2013. Replacement of Oct4 by Tet1 during iPSC induction reveals an important role of DNA methylation and hydroxymethylation in reprogramming. Cell Stem Cell 12, 453–469.

Graham, V., Khudyakov, J., Ellis, P., Pevny, L., 2003. SOX2 functions to maintain neural progenitor identity. Neuron 39, 749–765.

Han, J., Yuan, P., Yang, H., Zhang, J., Soh, B.S., Li, P., Lim, S.L., Cao, S., Tay, J., Orlov, Y.L., Lufkin, T., Ng, H.H., Tam, W.L., Lim, B., 2010. Tbx3 improves the germ-line competency of induced pluripotent stem cells. Nature 463, 1096–1100.

Han, D.W., Greber, B., Wu, G., Tapia, N., Arauzo-Bravo, M.J., Ko, K., Bernemann, C., Stehling, M., Scholer, H.R., 2011. Direct reprogramming of fibroblasts into epiblast stem cells. Nat. Cell Biol. 13, 66–71.

Han, D.W., Tapia, N., Hermann, A., Hemmer, K., Hoing, S., Arauzo-Bravo, M.J., Zaehres, H., Wu, G., Frank, S., Moritz, S., Greber, B., Yang, J.H., Lee, H.T., Schwamborn, J.C., Storch, A., Scholer, H.R., 2012. Direct reprogramming of fibroblasts into neural stem cells by defined factors. Cell Stem Cell 10, 465–472.

Hanna, J., Markoulaki, S., Schorderet, P., Carey, B.W., Beard, C., Wernig, M., Creyghton, M.P., Steine, E.J., Cassady, J.P., Foreman, R., Lengner, C.J., Dausman, J.A., Jaenisch, R., 2008. Direct reprogramming of terminally differentiated mature B lymphocytes to pluripotency. Cell 133, 250–264.

Hanna, J., Markoulaki, S., Mitalipova, M., Cheng, A.W., Cassady, J.P., Staerk, J., Carey, B.W., Lengner, C.J., Foreman, R., Love, J., Gao, Q., Kim, J., Jaenisch, R., 2009. Metastable pluripotent states in NOD-mouse-derived ESCs. Cell Stem Cell 4, 513–524.

Hemmer, K., Zhang, M., van Wullen, T., Sakalem, M., Tapia, N., Baumuratov, A., Kaltschmidt, C., Kaltschmidt, B., Scholer, H.R., Zhang, W., Schwamborn, J.C., 2014. Induced neural stem cells achieve long-term survival and functional integration in the adult mouse brain. Stem Cell Rep. 3, 423–431.

Hong, J.Y., Lee, S.H., Lee, S.C., Kim, J.W., Kim, K.P., Kim, S.M., Tapia, N., Lim, K.T., Kim, J., Ahn, H.S., Ko, K., Shin, C.Y., Lee, H.T., Scholer, H.R., Hyun, J.K., Han, D.W., 2014. Therapeutic potential of induced neural stem cells for spinal cord injury. J. Biol. Chem. 289, 32512–32525.

Huang, P., He, Z., Ji, S., Sun, H., Xiang, D., Liu, C., Hu, Y., Wang, X., Hui, L., 2011. Induction of functional hepatocyte-like cells from mouse fibroblasts by defined factors. Nature 475, 386–389.

Huangfu, D., Maehr, R., Guo, W., Eijkelenboom, A., Snitow, M., Chen, A.E., Melton, D.A., 2008. Induction of pluripotent stem cells by defined factors is greatly improved by small-molecule compounds. Nat. Biotechnol. 26, 795–797.

Ieda, M., Fu, J.D., Delgado-Olguin, P., Vedantham, V., Hayashi, Y., Bruneau, B.G., Srivastava, D., 2010. Direct reprogramming of fibroblasts into functional cardiomyocytes by defined factors. Cell 142, 375–386.

Kim, Y.J., Lim, H., Li, Z., Oh, Y., Kovlyagina, I., Choi, I.Y., Dong, X., Lee, G., 2014a. Generation of multipotent induced neural crest by direct reprogramming of human postnatal fibroblasts with a single transcription factor. Cell Stem Cell 15, 497–506.

Kim, S.M., Flasskamp, H., Hermann, A., Arauzo-Bravo, M.J., Lee, S.C., Lee, S.H., Seo, E.H., Lee, S.H., Storch, A., Lee, H.T., Scholer, H.R., Tapia, N., Han, D.W., 2014b. Direct conversion of mouse fibroblasts into induced neural stem cells. Nat. Protoc. 9, 871–881.

Li, K., Zhu, S., Russ, H.A., Xu, S., Xu, T., Zhang, Y., Ma, T., Hebrok, M., Ding, S., 2014. Small molecules facilitate the reprogramming of mouse fibroblasts into pancreatic lineages. Cell Stem Cell 14, 228–236.

Lu, J., Liu, H., Huang, C.T., Chen, H., Du, Z., Liu, Y., Sherafat, M.A., Zhang, S.C., 2013. Generation of integration-free and region-specific neural progenitors from primate fibroblasts. Cell Rep. 3, 1580–1591.

Maekawa, M., Yamaguchi, K., Nakamura, T., Shibukawa, R., Kodanaka, I., Ichisaka, T., Kawamura, Y., Mochizuki, H., Goshima, N., Yamanaka, S., 2011. Direct reprogramming of somatic cells is promoted by maternal transcription factor Glis1. Nature 474, 225–229.

Margariti, A., Winkler, B., Karamariti, E., Zampetaki, A., Tsai, T.N., Baban, D., Ragoussis, J., Huang, Y., Han, J.D., Zeng, L., Hu, Y., Xu, Q., 2012. Direct reprogramming of fibroblasts into endothelial cells capable of angiogenesis and reendothelialization in tissue-engineered vessels. Proc. Natl. Acad. Sci. U. S. A. 109, 13793–13798.

Mathieu, J., Zhou, W., Xing, Y., Sperber, H., Ferreccio, A., Agoston, Z., Kuppusamy, K.T., Moon, R.T., Ruohola-Baker, H., 2014. Hypoxia-inducible factors have distinct and stage-specific roles during reprogramming of human cells to pluripotency. Cell Stem Cell 14, 592–605.

Mikkelsen, T.S., Hanna, J., Zhang, X., Ku, M., Wernig, M., Schorderet, P., Bernstein, B.E., Jaenisch, R., Lander, E.S., Meissner, A., 2008. Dissecting direct reprogramming through integrative genomic analysis. Nature 454, 49–55.

Pijnappel, W.W., Esch, D., Baltissen, M.P., Wu, G., Mischerikow, N., Bergsma, A.J., van der Wal, E., Han, D.W., Bruch, H., Moritz, S., Lijnzaad, P., Altelaar, A.F., Sameith, K., Zaehres, H., Heck, A.J., Holstege, F.C., Scholer, H.R., Timmers, H.T., 2013. A central role for TFIID in the pluripotent transcription circuitry. Nature 495, 516–519.

Redmer, T., Diecke, S., Grigoryan, T., Quiroga-Negreira, A., Birchmeier, W., Besser, D., 2011. E-cadherin is crucial for embryonic stem cell pluripotency and can replace OCT4 during somatic cell reprogramming. EMBO Rep. 12, 720–726.

Ring, K.L., Tong, L.M., Balestra, M.E., Javier, R., Andrews-Zwilling, Y., Li, G., Walker, D., Zhang, W.R., Kreitzer, A.C., Huang, Y., 2012. Direct reprogramming of mouse and human fibroblasts into multipotent neural stem cells with a single factor. Cell Stem Cell 11, 100–109.

Schnabel, L.V., Abratte, C.M., Schimenti, J.C., Southard, T.L., Fortier, L.A., 2012. Genetic background affects induced pluripotent stem cell generation. Stem Cell Res. Ther. 3, 30.

Sekiya, S., Suzuki, A., 2011. Direct conversion of mouse fibroblasts to hepatocyte-like cells by defined factors. Nature 475, 390–393.

Shi, Y., Do, J.T., Desponts, C., Hahm, H.S., Scholer, H.R., Ding, S., 2008. A combined chemical and genetic approach for the generation of induced pluripotent stem cells. Cell Stem Cell 2, 525–528.

Singhal, N., Graumann, J., Wu, G., Arauzo-Bravo, M.J., Han, D.W., Greber, B., Gentile, L., Mann, M., Scholer, H.R., 2010. Chromatin-remodeling components of the BAF complex facilitate reprogramming. Cell 141, 943–955.

Son, E.Y., Ichida, J.K., Wainger, B.J., Toma, J.S., Rafuse, V.F., Woolf, C.J., Eggan, K., 2011. Conversion of mouse and human fibroblasts into functional spinal motor neurons. Cell Stem Cell 9, 205–218.

Subramanyam, D., Lamouille, S., Judson, R.L., Liu, J.Y., Bucay, N., Derynck, R., Blelloch, R., 2011. Multiple targets of miR-302 and miR-372 promote reprogramming of human fibroblasts to induced pluripotent stem cells. Nat. Biotechnol. 29, 443–448.

Takahashi, K., Yamanaka, S., 2006. Induction of pluripotent stem cells from mouse embryonic and adult fibroblast cultures by defined factors. Cell 126, 663–676.

Wang, L., Wang, L., Huang, W., Su, H., Xue, Y., Su, Z., Liao, B., Wang, H., Bao, X., Qin, D., He, J., Wu, W., So, K.F., Pan, G., Pei, D., 2013. Generation of integration-free neural progenitor cells from cells in human urine. Nat. Methods 10, 84–89.

Yoshida, Y., Takahashi, K., Okita, K., Ichisaka, T., Yamanaka, S., 2009. Hypoxia enhances the generation of induced pluripotent stem cells. Cell Stem Cell 5, 237–241.

Yu, B., He, Z.Y., You, P., Han, Q.W., Xiang, D., Chen, F., Wang, M.J., Liu, C.C., Lin, X.W., Borjigin, U., Zi, X.Y., Li, J.X., Zhu, H.Y., Li, W.L., Han, C.S., Wangensteen, K.J., Shi, Y., Hui, L.J., Wang, X., Hu, Y.P., 2013. Reprogramming fibroblasts into bipotential hepatic stem cells by defined factors. Cell Stem Cell 13, 328–340.

Yu, K.R., Shin, J.H., Kim, J.J., Koog, M.G., Lee, J.Y., Choi, S.W., Kim, H.S., Seo, Y., Lee, S., Shin, T.H., Jee, M.K., Kim, D.W., Jung, S.J., Shin, S., Han, D.W., Kang, K.S., 2015. Rapid and efficient direct conversion of human adult somatic cells into neural stem cells by HMGA2/let-7b. Cell Rep.

Zhu, S., Ambasudhan, R., Sun, W., Kim, H.J., Talantova, M., Wang, X., Zhang, M., Zhang, Y., Laurent, T., Parker, J., Kim, H.S., Zaremba, J.D., Saleem, S., Sanz-Blasco, S., Masliah, E., McKercher, S.R., Cho, Y.S., Lipton, S.A., Kim, J., Ding, S., 2014. Small molecules enable OCT4-mediated direct reprogramming into expandable human neural stem cells. Cell Res. 24, 126–129.